International Journal of Biochemistry and Cell Biology 108 (2019) 72–83

Contents lists available at ScienceDirect

International Journal of Biochemistry and Cell Biology

journal homepage: www.elsevier.com/locate/biocel

Tri-block copolymer nanoparticles modified with folic acid for temozolomide delivery in glioblastoma

Soraya Emamgholizadeh Minaei[a], Samideh Khoei[a,*], Sepideh Khoee[b], Mohammad Reza karimi[b]

[a] Department of Medical Physics, School of Medicine, Iran University of Medical Sciences, Tehran, Iran
[b] Department of Polymer Chemistry, School of Chemistry, College of Science, University of Tehran, Tehran, Iran

ARTICLE INFO

Keywords:
Glioblastoma multiforme
Temozolomide
Drug delivery
Folic acid
Nanoparticles

ABSTRACT

In the present study, Folic Acid (FA) ligand was used to functionalize Temozolomide-loaded Poly (ethylene Glycol)–Poly (Butylene Adipate)–Poly (ethylene Glycol)-coated magnetite nanoparticles (TMZ-SPION-PEG-PBA-PEG) for targeted chemotherapy of glioma cells.

Four types of nanoparticles were synthesized with the hydrodynamic diameters of 24–49 nm. Using MTT, Prussian blue, and ICP-OES assays, the cytotoxicity effect and cellular uptake of nanoparticles were evaluated in C6 cancer cells and OLN-93 normal cells. Moreover, in vitro anti-tumor efficacy of nanoparticles was evaluated through colony formation, quantitative real-time PCR, and flow cytometry analysis.

As compared to OLN-93 cells TMZ-SPION-PEG-PBA-PEG-FA nanoparticles showed an increase in the cytotoxicity of the loaded TMZ in C6 cells within 24 and 48 h treatment ($P < 0.0001$), while such effect was not observed in the case of non-targeting nanoparticles. The colony formation, flow cytometry, and real-time PCR assays showed that TMZ-SPION-PEG-PBA-PEG-FA led to the enhancement of inhibitory effects to C6 cells compared to TMZ alone ($P < 0.05$).

These results suggested that TMZ-SPION-PEG-PBA-PEG-FA could effectively slow down cell proliferation, due to the targeting effect and the high accumulation of TMZ in C6 cells via an FA-receptor mediated endocytosis. In conclusion, TMZ-loaded magnetite FA-conjugated PEG-PBA-PEG NPs could be used as a targeted drug delivery system for targeted therapy of brain glioma.

1. Introduction

Nowadays, glioblastoma multiforme (GBM), a grade of IV astrocytoma is the most frequent primary malignant tumor of the brain, which accounts for about 42% of all primary brain tumors (Kim and Lee, 2009; Wen and Kesari, 2008). However, due to the highly proliferative and infiltrative nature of GBM, its treatment is one of the most challenging problems in cancer therapy. Also, the presence of invasive cancer cells in the adjacent normal brain parenchyma cause to relapse at the site of the primary tumor (Gladson et al., 2010; Furnari et al., 2007).

Temozolomide (TMZ) is one of the most common antineoplastic agents that are used as a first drug for the treatment of malignant glial tumor (Reni et al., 2004; Tsang et al., 1991). However, the clinical outcome in the treatment of GBM is disappointing due to the poor drug penetration across the blood-brain barrier (BBB), the short half-life of approximately 1.8 h in plasma, dose-limiting side effects, non-targeted and non-specific nature of TMZ (Baker et al., 1999; Sarin, 2009). In order to overcome these deficiencies, a targeted drug delivery system (TDDS) based on biodegradable polymeric nanoparticle (NP) carriers has received attention for carrying bioactive compound in the body and improving its safety and efficacy (Karlsson et al., 2018; Rychahou et al., 2018).

Amphiphilic block copolymers have been broadly used in DDS. In the context, biodegradable and biocompatible triblock copolymer poly (ethylene glycol)-poly (butylene adipate)-poly (ethylene glycol) (PEG-PBA-PEG) has been developed to improve the therapeutic efficacy of drugs at the target site. The hydrophilic shell protects NPs from being recognized and eliminated by the reticuloendothelial system (RES). Therefore, they lead to a higher stability in biological fluids and increase blood circulation time, but hydrophobic core can be loaded by lipophilic drugs such as TMZ to preserve them from aqueous medium and degradation, also it can control and sustain drug release (Özcan et al., 2010; Khoei et al., 2012).

Due to small size of NPs ranging from 10 nm to 100 nm, they can specifically accumulate in tumor via a passive targeting device known

* Corresponding author at: Department of Medical Physics, School of Medicine, Iran University of Medical Sciences, P.O.Box: 1449614525, Tehran, Iran.
E-mail addresses: khoei.s@iums.ac.ir, skhoei@gmail.com (S. Khoei).

https://doi.org/10.1016/j.biocel.2019.01.010
Received 7 October 2018; Received in revised form 14 January 2019; Accepted 16 January 2019
Available online 17 January 2019
1357-2725/

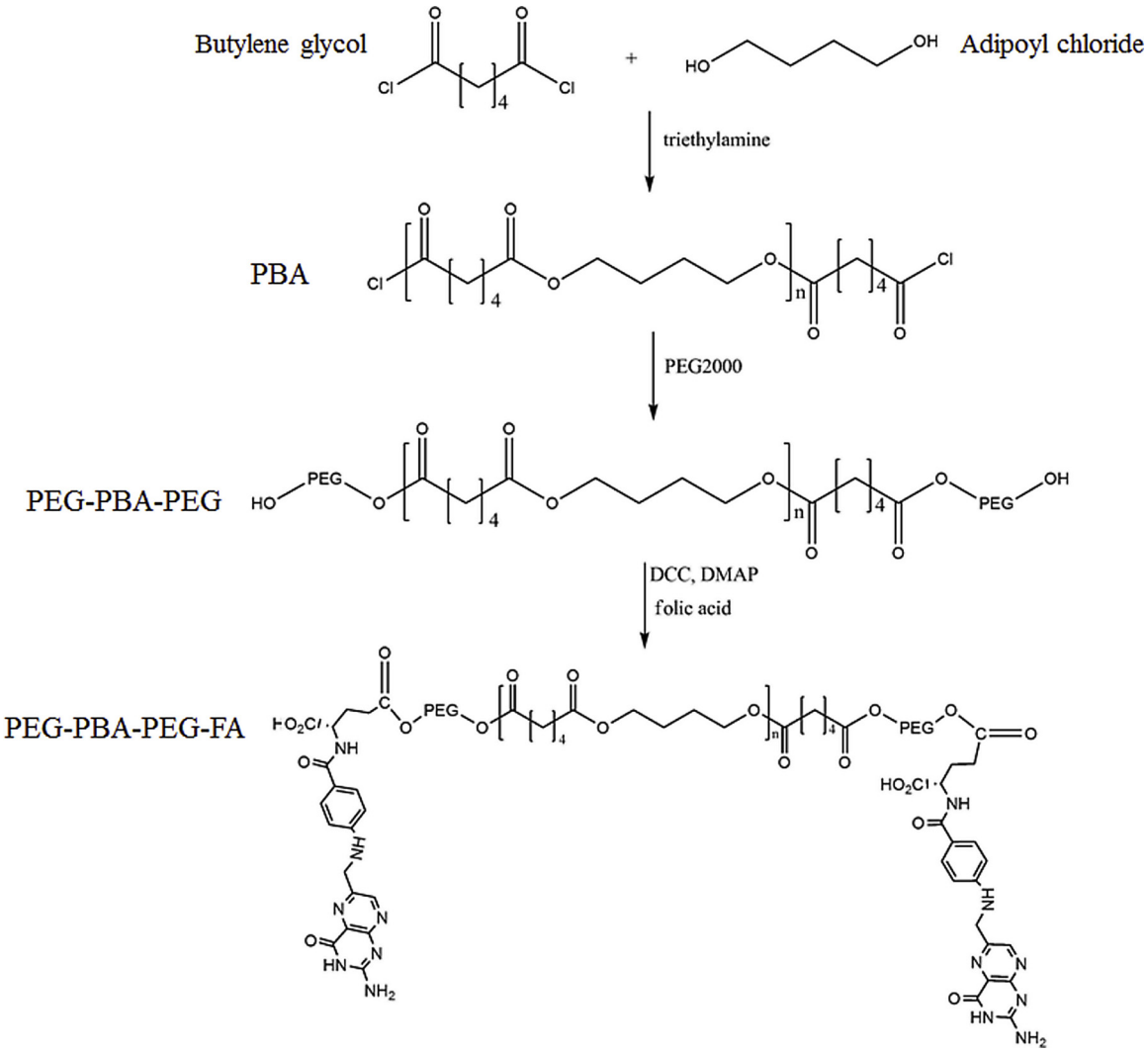

Scheme 1. The chemical synthesis of PEG-PBA-PEG and PEG-PBA-PEG-FA triblock copolymers.

as enhanced permeability and retention (EPR) effect (Cherukuri et al., 2010). Moreover, active targeting minimizes off-target drug accumulation with a tumor-specific ligand that selectively binds to receptors that are over-expressed on the tumor cells, (Cheng et al., 2017; Miura et al., 2013). Folic acid (FA) ligand can preferably associate with folate-receptor (FR) that is generally over-expressed on the most type of cancer cells such as GBM, breast, and ovarian cancers while only minimally distributed in normal cells (Kuo and Chen, 2015; Erdoğar et al., 2018; Jaimes-Aguirre et al., 2017).

Superparamagnetic iron oxide nanoparticles (SPIONs) have been developed as a powerful tool in medicine. They can be used for detection (Hadjipanayis et al., 2010; Shanavas et al., 2017; Mohammadi Gazestani et al., 2018), tracing of nanoparticles (Kargar et al., 2018; Mustafa et al., 2013), and treatment of cancer cells (Asadi et al., 2018).

In order to justify this hypothesis, SPION-PEG-PBA-PEG nanoparticles were designed and loaded with TMZ as a chemotherapeutic agent and its surface was functionalized with folic acid for improving cellular uptake. Physical characterization of NPs had been evaluated to ensure the size range and other physical properties. Moreover, in vitro efficacy of NPs delivery, cellular uptake and the cytotoxic effects were evaluated against the monolayer culture of C6 glioma cells and OLN-93 glial cells.

2. Materials and methods

2.1. Materials

Poly (ethylene glycol) (PEG, *Mw* = 2000), Poly (butylene adipate) (PBA), adipoyl chloride, triethylamine, butylene glycol, diethyl ether, iron (II) chloride tetrahydrate (FeCl2.4H2O), iron (III) chloride hexahydrate (FeCl3.6H2O), dimethylformamide (DMF), dichloromethane (DCM), were obtained from Merck Chemical Company (Darmstadt, Germany). Temozolomide (TMZ), folic acid, *N,N'*-Dicyclohexylcarbodiimide (DCC), 4-dimethylamino pyridine (DMAP), 3-(4,5-dimethyl-thiazol-2-yl)-2,5- diphenyl-tetrazolium bromide (MTT), potassium ferrocyanide (II) trihydrate, Formaldehyde solution, dimethyl sulfoxide (DMSO), trypsin and EDTA were purchased from Sigma Chemical Company (St. Louis, MO, USA). Fetal Bovine Serum (FBS), penicillin-streptomycin were purchased from Biowest. Dulbecco's modified Eagle's medium (DMEM), and Ham's F12 were purchased from Gibco (Invitrogen, USA). Annexin V-FITC apoptosis detection kit was purchased from eBioscience (San Diego, USA). cDNA synthesis kit and SYBR Green qPCR Master Mix were obtained from Takara (Takara Bio Inc., Japan). In addition, the C6 and OLN-93 cell lines were provided from Pasteur Institute of Iran.

2.2. Preparation of nanoparticles

2.2.1. Synthesis of triblock copolymers (PEG-PBA-PEG)

Polycondensation method was used to synthesize PEG–PBA–PEG. In a 10-mL round-bottom flask equipped with a magnetic stirrer, 2.48 mL (16.9 mmol) adipoyl chloride, 0.91 mL (16.1 mmol) butylene glycol, and 4×10^{-2} mL triethylamine were heated at 85°C for 24 h until no more hydrochloric acid (HCL) was released. Acid chloride terminated poly (butylene adipate) (PBA) was prepared in this step. Then, an excess amount of PEG (2000) was added to PBA and the reaction was continued at the same temperature for 24 h. The resulting copolymers were precipitated in 40 mL diethyl ether at 15°C and washed three times with deionized water. Finally, white triblock copolymers were separated by centrifugation.

2.2.2. Folic acid coupling with PEG-PBA-PEG

100 mg of folic acid powder was dissolved in 10 mL DMF in a round-bottom flask equipped with a magnetic stirrer, and then 42 mg DCC and 25 mg DMAP were added to the solution. Afterward, for activation of folic acid, the solution was stirred at room temperature for 4 h, which was followed by addition of 1 g of tri-block copolymers (PEG-PBA-PEG) to the solution and the reaction was continued overnight under the dark condition.

As well as, the product was precipitated in 100 mL diethyl ether and dissolved in DCM twice to remove impurities from the obtained product. In addition, excessive folic acid was separated from the product by centrifugation. Subsequently, the resultant product was precipitated in diethyl ether and then dried at room temperature for 24 h (Scheme 1).

2.2.3. Preparation of drug-loaded magnetite nanoparticles (TMZ-SPION-PEG-PBA-PEG-FA)

TMZ-loaded magnetite FA-conjugated PEG-PBA-PEG nanoparticles were synthesized according to the nanoprecipitation method. Superparamagnetic iron oxide nanoparticles (SPIONs) were synthesized by the co-precipitation method according to Khoee et al. report (Khoee et al., 2015). 20 mg of SPION (Fe_3O_4) was dispersed in 2 mL of acetone using an ultrasonic bath, and then 50 mg of FA-conjugated PEG-PBA-PEG copolymer was added to the solution and followed by addition of 0.5 mL of DMSO solution containing 10 mg of TMZ. After that, at the time of stirring, the solution was added drop by drop to 20 mL of deionized water.

Using reduced pressure, the acetone was removed from the solution and the nanoparticles were coated with the polymer. Afterward, the nanoparticles were washed once with the acetone and deionized water, respectively. Finally, the nanoparticles were dried using a freezing dryer. TMZ-SPION-PEG-PBA-PEG nanoparticles were prepared in a similar way, while triblock copolymer without FA-ligand was added to the solution. Moreover, drug-free nanoparticles (SPION-PEG-PBA-PEG and SPION- PEG-PBA-PEG-FA) were also obtained in the same way without incorporating the drug in the process.

2.3. Nuclear magnetic resonance analysis of tri-block copolymers

In order to evaluate the composition of the synthesized copolymer and the folic acid binding to the tri-block copolymer, the 1H Nuclear Magnetic Resonance (NMR) analysis was performed on PEG-PBA-PEG tri-block copolymer with and without folic acid ligand using a Varian Inova, 500 MHz, 1H NMR spectroscopy. Samples were dissolved in deuterated chloroform ($CDCl_3$) and their spectra were obtained.

2.4. Carbon-hydrogen-nitrogen (CHN) elemental analysis

In order to confirm the presence of TMZ in nanoparticles, CHN elemental analysis was carried out on SPION-PEG-PBA-PEG-FA nanoparticles with and without Temozolomide drug using a CHN elemental analyzer (Flash EA 1112 series, Thermo Finnigan).

2.5. Characterization of the nanoparticles

2.5.1. Particle size, zeta potential, and the morphology of nanoparticles

Mean hydrodynamic size, size distribution, and zeta potential of NPs (SPION-PEG-PBA-PEG, SPION-PEG-PBA-PEG-FA, TMZ-SPION-PEG-PBA-PEG, and TMZ-SPION-PEG-PBA-PEG-FA) were determined by Dynamic Light Scattering (DLS) analysis using a Zeta Potential/Particle Sizer (Nanoflex, Particle Metrix, Germany). The samples were diluted with deionized water to an appropriate concentration and sonicated for 10 min before measurement.

The morphology of NPs was characterized using a Transmission Electron Microscope (TEM) (Zeiss LEO906, Jena, Germany). Nanoparticles were dispersed in deionized water and then sonicated for 10 min A drop of the dispersed samples was mounted on a carbon-coated copper grid. Then, the grid was observed under the TEM with an accelerating voltage of 100 kV.

2.5.2. Encapsulation efficiency and drug loading capacity

To investigate the drug loading capacity and encapsulation efficiency, 2 mg of TMZ- incorporated NPs (TMZ-SPION-PEG-PBA-PEG and TMZ-SPION-PEG-PBA-PEG-FA) were dissolved in acetone and the concentration of TMZ was measured using a UV-spectrophotometer (Ultraospec 3000, Pharmacia Biotech, USA) at a wavelength of 329 nm (characteristic absorption band of TMZ). The Drug Loading Capacity (DLC) and Encapsulation Efficiency (EE) were determined according to equation 1 and 2:

$$DLC\ (\%) = \frac{Amount\ of\ TMZ\ in\ the\ nanoparticles}{nanoparticles\ weight} \times 100 \quad (1)$$

$$EE\ (\%) = \frac{Amount\ of\ TMZ\ in\ the\ nanoparticles}{Total\ amount\ of\ TMZ\ in\ the\ initial\ loading} \times 100 \quad (2)$$

2.5.3. In vitro TMZ release profiles

The equilibrium dialysis bag diffusion method was used to evaluate the in vitro release behaviors of TMZ from NPs (TMZ-SPION-PEG-PBA-PEG and TMZ-SPION-PEG-PBA-PEG-FA). The weighed amount of TMZ alone and both NPs was suspended in Phosphate Buffer Saline (PBS) and transferred into a dialysis bag (MWCO 12,400 Da). Then, the dialysis bag was submerged fully into 10 mL release medium (PBS) under pH = 7.4 and incubated at 37 °C at the shaking speed of 100 rpm. At pre-determined time intervals, the entire media was taken out and replaced with an equal volume of fresh media. The released TMZ concentration was measured using an UV-spectrophotometer at 329 nm.

2.6. Cell experiments

2.6.1. Cell culture

The C6 rat glioblastoma and OLN-93 rat glial cell lines were obtained from Pasteur Institute of Iran and cultured in medium (Ham's F12 for C6 and DMEM for OLN-93) supplemented with 10% FBS, 100 U/mL penicillin and 100 mg/mL streptomycin at 37 °C under 5% CO2 and 95% air humidified environment incubator at a density of 10 (Furnari et al., 2007) cells/cm (Wen and Kesari, 2008). All experiments were done in the logarithmic phase of the cell growth.

2.6.2. Cellular uptake of NPs

2.6.2.1. Prussian blue staining. The cellular uptake of NPs (intracellular ferric iron) was measured using the Prussian blue staining assay. The C6 and OLN-93 cell lines were seeded in 6-well plates and incubated for 24 h. After that, the medium was changed for both cell lines and continued to incubate with 0.493 mg/mL of SPION-PEG-PBA-PEG or SPION-PEG-PBA-PEG-FA NPs for 2 h and 24 h with the same concentrations of Fe_3O_4 (0.123 mg/mL). Then, the cells were washed with PBS for three times, fixed with 4% paraformaldehyde solution for 20 min, stained with the Prussian blue solution (comprised equal

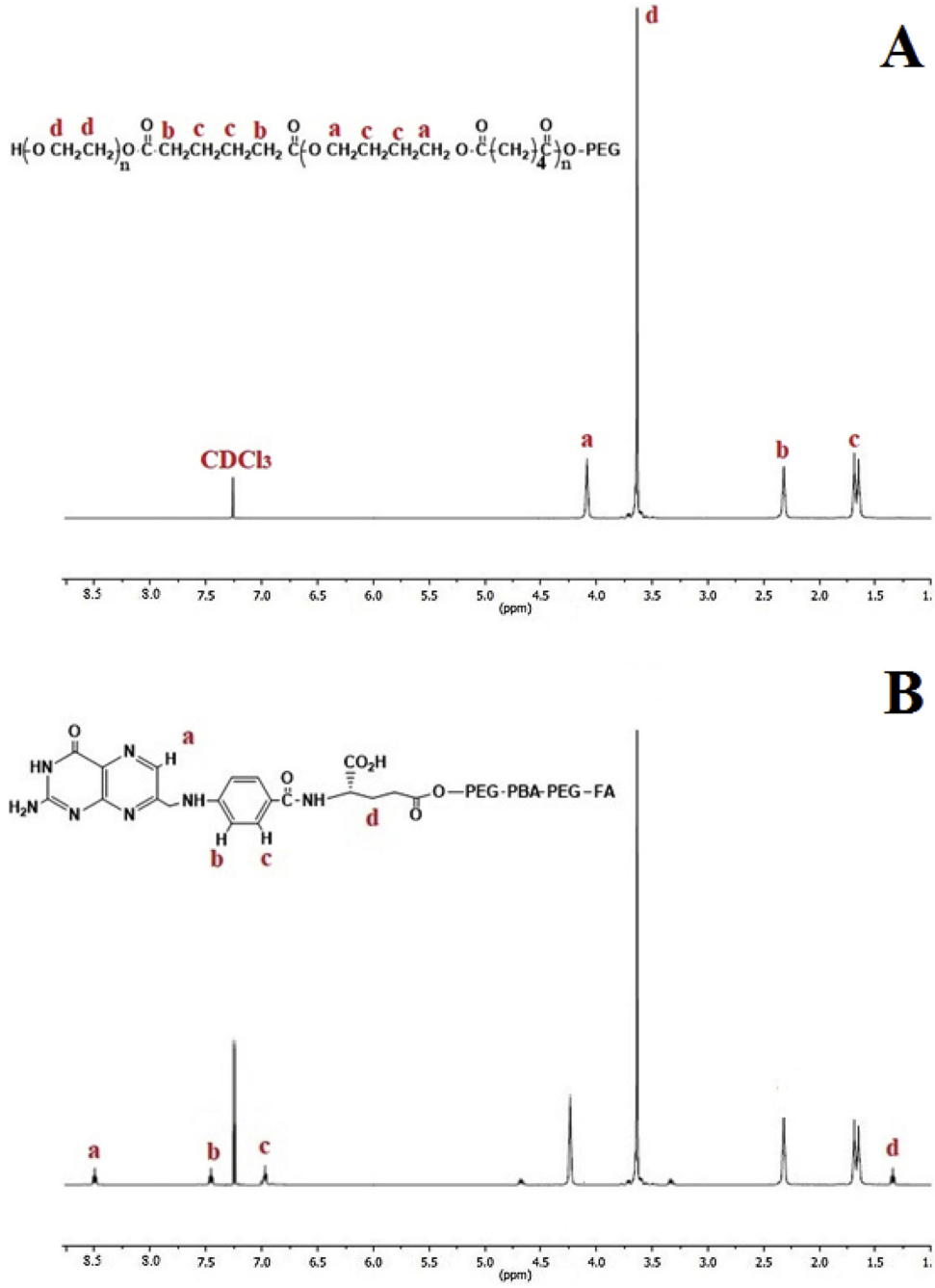

Fig. 1. 1H-NMR spectrum of (A) PEG–PBA–PEG triblock copolymer and (B) FA-conjugated PEG–PBA–PEG triblock copolymer (Deuterated chloroform ($CDCl_3$) is a solvent used for the NMR analysis).

Table 1
CHN elemental analysis of folic acid-conjugated nanoparticles with and without temozolomide drug.

Samples	Carbon (%)	Hydrogen (%)	Nitrogen (%)
SPION-PEG-PBA-PEG-FA	40.92	6.22	3.36
TMZ-SPION-PEG-PBA-PEG-FA	41.13	6.09	7.04

volume of 2% potassium ferrocyanide (II) trihydrate and 2% hydrochloric acid) for 30 min, washed with PBS, and imaged using an optical microscope at the magnification of 400X (Olympus CK2; Olympus Optical Co., Tokyo, Japan).

2.6.2.2. Quantitation of the uptake of NPs using an inductively coupled plasma optical emission spectrometry (ICP-OES). Both cell lines were cultured in T-25 cell culture flasks at a density of 2 × 10 (Tsang et al., 1991) cells, incubated for 24 h and then treated in the same way as described in section 2.6.2.1. After treatment, the cells were washed with PBS to remove the free nanoparticles in the media, detached from the flask using trypsin, and counted for quantification purposes. The cells were digested with 1 mL of concentrated HNO_3 at 150 °C for 2 h. The samples were diluted to 5 mL with deionized water and the concentration of iron was measured using an ICP-OES assay (VISTA-PRO, Varian, Australia). Finally, the average iron content per cell was calculated.

2.6.3. In vitro cytotoxicity assay

The cytotoxicity of the four types of NPs and TMZ alone was

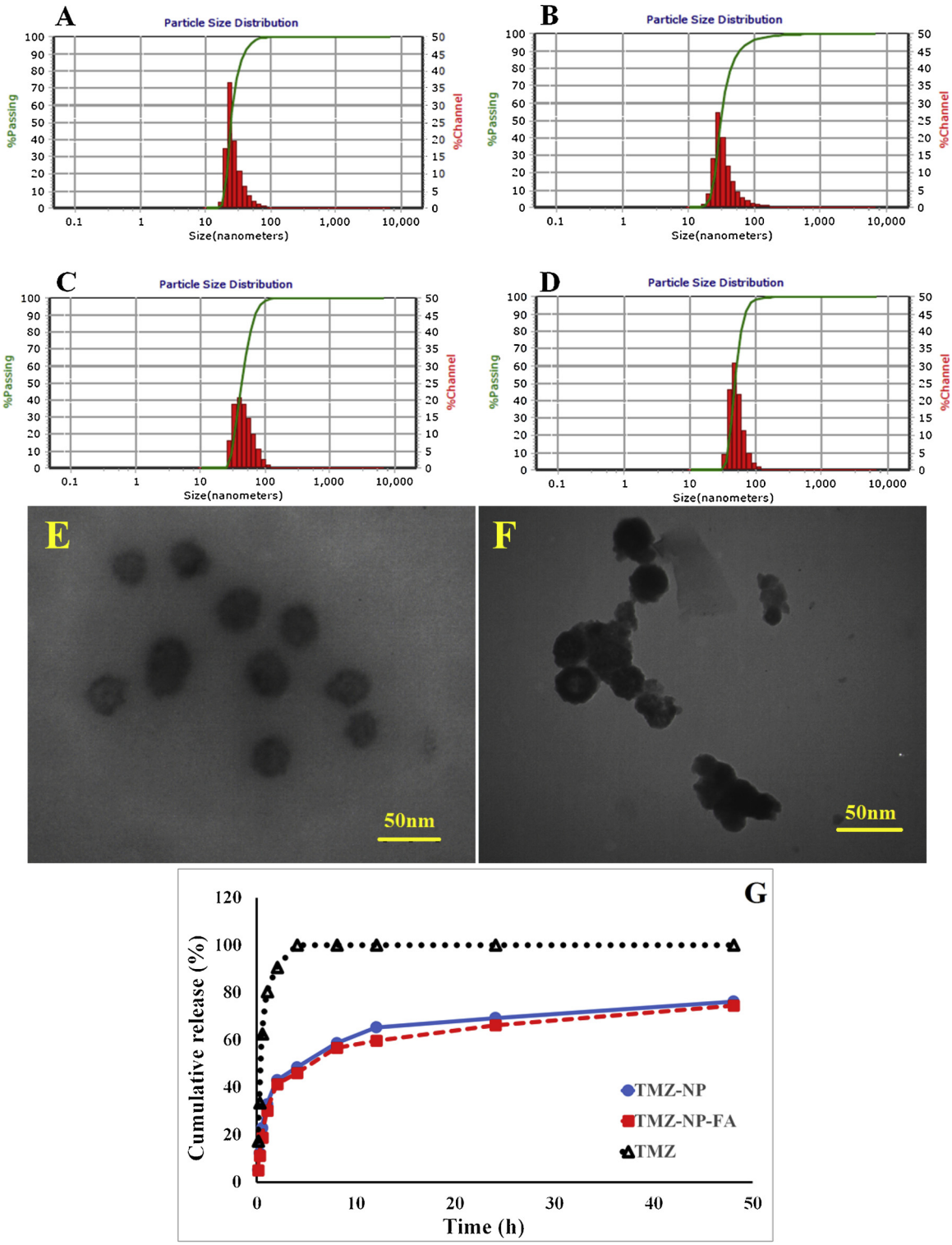

Fig. 2. Characterization of nanoparticles. Particle size distributions of (A) SPION-PEG-PBA-PEG, (B) SPION-PEG-PBA-PEG-FA, (C) TMZ-SPION-PEG-PBA-PEG, and (D) TMZ-SPION-PEG-PBA-PEG-FA. TEM images of (E) TMZ-SPION-PEG-PBA-PEG and (F) TMZ-SPION-PEG-PBA-PEG-FA. (G) In vitro TMZ release profiles in PBS (pH 7.4) at 37 °C (NP means SPION-PEG-PBA-PEG).

evaluated using MTT assay. The C6 and OLN-93 cell lines were seeded in a 96-well plate (15 × 10 (Gladson et al., 2010) cells/well). After 24 h, the cells were treated for 24 and 48 h with TMZ and different types of NPs (SPION-PEG-PBA-PEG, SPION-PEG-PBA-PEG-FA, TMZ-SPION-PEG-PBA-PEG, or TMZ-SPION-PEG-PBA-PEG-FA) at equivalent TMZ concentrations ranging from 3.9 to 500 μg/mL. After treatment, all wells were washed twice with PBS, then 20 μL of MTT solution (5 mg/mL) was added to each well, and continued to incubate for an additional 4 h. Subsequently, the medium containing MTT was removed, 100 μL of dimethyl sulfoxide (DMSO) was added to each well to dissolve any formed purple formazan crystals. After shaking for 10 min, the absorbance (570 nm-test/630 nm-reference) was measured using a microplate reader (BioTek, USA). The percentage of viable cells at each concentration was calculated according to equation 3 and plotted as a

Table 2
The characterizations of nanoparticles.

Nanoparticles	Size (nm)	Zeta Potential (mV)	DLC%	EE%
SPION-PEG-PBA-PEG	24.82	−37.1 ± 0.54	–	–
SPION-PEG-PBA-PEG-FA	27.33	−28.45 ± 0.22	–	–
TMZ-SPION-PEG-PBA-PEG	44	−30.05 ± 0.57	6.3	50
TMZ-SPION-PEG-PBA-PEG-FA	48.6	−27.92 ± 0.32	6.65	52.8

function of TMZ concentrations.

$$cellviability(\%) = \frac{\text{Absorbance value oftreatedcells}}{\text{Absorbance value of control(untreated)cell}} \times 100 \quad (3)$$

2.6.4. In vitro anti-tumor efficacy of nanoparticles

2.6.4.1. Colony formation assay. Colony formation assay was used to evaluate the long-term cytotoxicity of TMZ and NPs. The C6 cell line at a density of 4 × 10 (Reni et al., 2004) were seeded in T-25 cell culture flasks. After 24 h incubation, the cells were treated with 111.7 µM of TMZ (21.7 µg/mL), 0.493 mg/mL of TMZ-SPION-PEG-PBA-PEG-FA (containing 111.7 µM of TMZ), and 0.493 mg/mL of SPION-PEG-PBA-PEG-FA NPs for 24 and 48 h. Then, the treated and control cells were washed with PBS and harvested. Single cell suspensions were seeded in 60 mm Petri dishes and incubated in the presence of Ham's F12, supplemented with 10% FBS for a period of 6 days. The cells were fixed using 4% Formaldehyde in PBS and stained with 0.5% Crystal violet. The colonies were counted using an optical microscope and the plating efficiency (PE) was determined by Eq. (4).

$$PE\ (\%) = \frac{Number\ of\ the\ colony}{Number\ of\ cell - seeded} \times 100 \quad (4)$$

2.6.4.2. Quantitative real-time PCR. The C6 cells were treated with TMZ, TMZ-SPION-PEG-PBA-PEG-FA, and SPION-PEG-PBA-PEG-FA for 24 h in the same way as described above. The treated cells along with negative control cells were trypsinized, and approximately 3 × 10 (Tsang et al., 1991) cells were collected. Then, total RNA was extracted for each sample using RNX-plus reagent (CinnaGen, Iran) according to the manufacturer's instructions. RNA concentration and its purity were determined using a NanoDrop One Spectrophotometer (Thermo Scientific, USA). Moreover, for checking the integrity of RNA, extracted RNA was applied on 1.5% agarose gel to observe 18 s and 28 s bands. After that, 2 µg of total RNA was reversely transcribed to cDNA using the cDNA Synthesis kit (Takara Bio Inc., Japan) according to the manufacturer's operating instructions. Quantitative real-time PCR (qPCR) amplifications were performed using SYBR Green qPCR Master Mix (Takara Bio Inc., Japan) in a real-time PCR system (Rotorgene-Q, Germany) and the reaction conditions were included: initial denaturation at 95 °C for 30 s, followed by 40 cycles of denaturation at 95 °C for 5 s, and annealing/ extension at 60 °C for 35 s. The primer sequences were:

Bax
F: 5′-CGATGAACTGGACAACAACATGG-3′
R: 5´-GCAAAGTAGAAAAGGGCAACCAC-3′
Bcl-2
F: 5′-AGGATTGTGGCCTTCTTTGAGTT-3′
R: 5′-GCCGGTTCAGGTACTCAGTCAT-3′
Housekeeping gene GAPDH
F: 5´-AGTTCAACGGCACAGTCAAG-3´
R: 5´-TACTCAGCACCAGCATCACC-3´

The cycle threshold (Ct) values in each sample for all primers were determined and the ΔΔCt values were calculated using equation 5:

((5)) $\Delta\Delta Ct = (Ct_{\text{sample}} - Ct_{\text{reference gene}}) - (Ct_{\text{negative control}} - Ct_{\text{reference gene}})$

After standardization, the $2^{-\Delta\Delta Ct}$ values for Bax and Bcl-2 primers were calculated. Then, the relative Bax/Bcl-2 mRNA expression values were reported.

2.6.4.3. Cell apoptosis assay. To evaluate the cell apoptosis induced by the TMZ and NPs, the C6 glioma cell line was cultured and treated in the same way as described in Section 2.6.4.1. After 24 h treatment, the treated and untreated cells were trypsinized, washed with ice-cold PBS and re-suspended in the 1X binding buffer at a concentration of 1–5 × 10 (Tsang et al., 1991) cells/mL. Thereafter, 5 µL of FITC Annexin-V was added to each sample and incubated for 15 min at room temperature under dark conditions. Before analyzing by flow cytometry, 5 µL of Propidium iodide (PI) was added to each sample and the fluorescence of cells was evaluated using a flow cytometer BD FACS Calibur (BD, San Jose, CA, USA). The percentage of cells undergoing apoptosis and necrosis in each sample was analyzed and calculated. The data were obtained by the average of triple measurements.

2.7. Statistical analysis

All experimental data were expressed as the mean ± standard deviation (SD) and analyzed by one-way analysis of variance (ANOVA) followed by Tukey's test as the post-hoc using SPSS version 16. P-values less than 0.05 were assumed to be significant.

3. Results

3.1. Nuclear magnetic resonance analysis of tri-block copolymers

The 1H NMR results were shown in Fig. 1. The methylene protons (H_d) of PEG segments of the copolymer was obvious at about 3.59 ppm. In addition, the PBA segment of the copolymer showed characteristic peaks of methylene protons (H_a, H_b, and H_c) at 1.67, 2.28, and 4.09 ppm (Fig. 1A). Moreover, Fig. 1B confirmed the attachment of the folic acid ligand onto tri-block copolymers. The 1H NMR spectrum of the PEG-PBA-PEG-FA nanoparticles showed other characteristic peaks that were attributed to the aromatic protons (H_a, H_b, H_c, and H_d) of the folic acid ligand.

3.2. CHN elemental analysis

According to CHN elemental analysis (Table 1), there was 3.36% nitrogen in the composition of the SPION-PEG-PBA-PEG-FA nanoparticles that was related to the folic acid ligand. In the TMZ-loaded nanoparticles, the amount of nitrogen element was increased to 7.04% that was belonged to temozolomide drug, which indicated that the drug has been loaded into nanoparticles.

3.3. Characterization of the nanoparticles

3.3.1. Particle size, zeta potential, and the morphology of nanoparticles

DLS measurements indicated that all nanoparticles had mean hydrodynamic diameters of 24–49 nm. The size, polydispersity index, and zeta potential of various NPs have been shown in Fig. 2A-D and Table 2. Moreover, the morphology of TMZ-SPION-PEG-PBA-PEG-FA and TMZ-SPION-PEG-PBA-PEG nanoparticles has been shown in Figure 2E&F. TEM analysis of TMZ-loaded NPs confirmed that nanoparticles possessed a spherical shape with a uniform particle size of about 40 nm which was slightly less than the size measured by DLS. This difference may be attributed to the absorption of liquid by the NPs during the DLS analysis.

3.3.2. Encapsulation efficiency and drug loading capacity

The TMZ encapsulation efficiency of TMZ-SPION-PEG-PBA-PEG-FA and TMZ-SPION-PEG-PBA-PEG nanoparticles were 52.8 and 50%, respectively, with the drug loading coefficient of 6.65 and 6.3%,

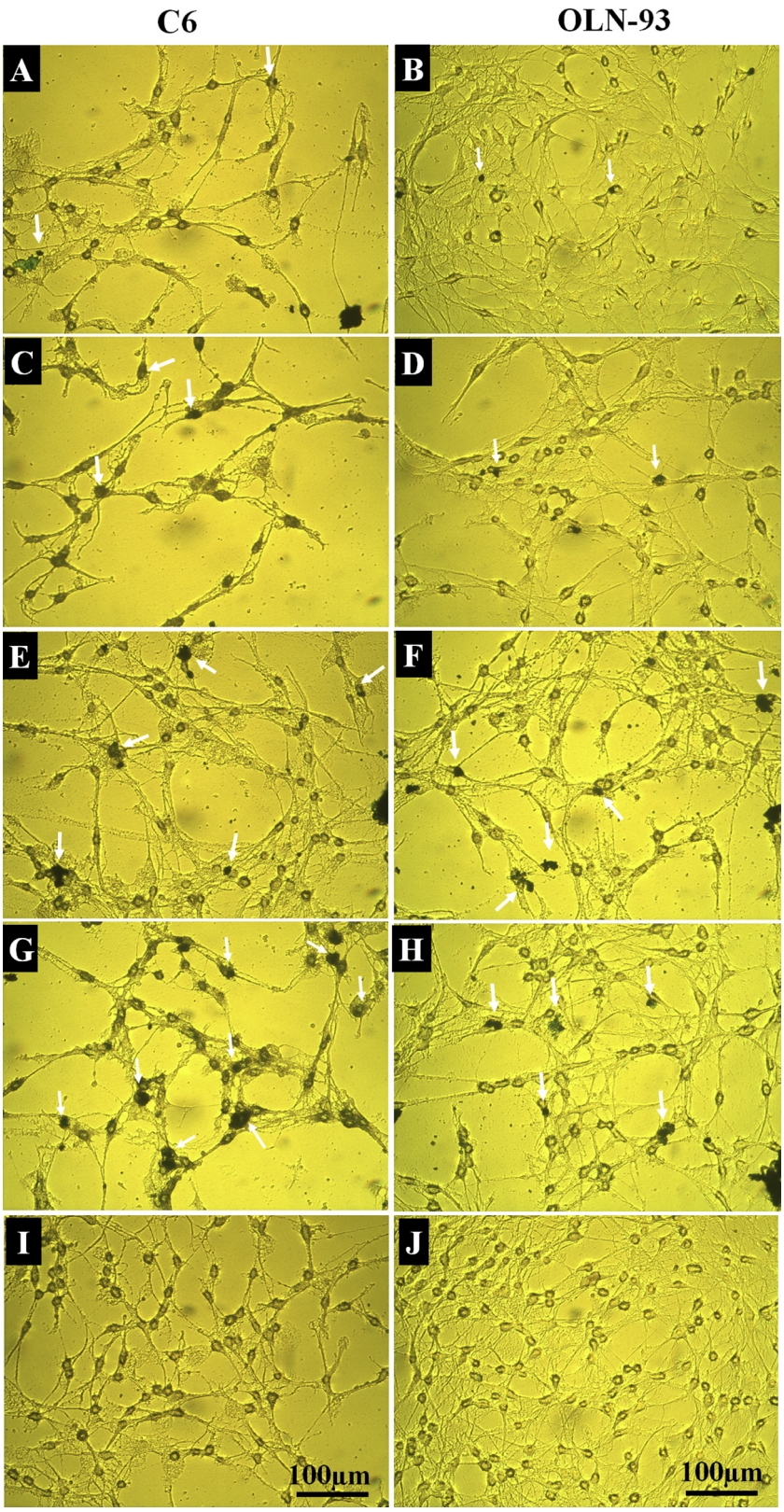

Fig. 3. Uptake of NPs by C6 and OLN-93 cells was determined using the Prussian blue assay. After the cells were treated with SPION-PEG-PBA-PEG (A&B) and SPION-PEG-PBA-PEG-FA (C&D) for 2 h. Also, treated with SPION-PEG-PBA-PEG (E&F) and SPION-PEG-PBA-PEG-FA (G&H) for 24 h. In this figure, control cells were also shown (I&J) (nanoparticles were indicated by white arrows, magnification 400x). (For interpretation of the references to colour in this figure legend, the reader is referred to the web version of this article).

Table 3
The amount of Fe taken up by C6 and OLN-93 cells after 24 h treatment was determined using the ICP-OES analysis (mean ± SD, n = 3).

Cell lines	Amount of Fe (pg/cell)	
	SPION-PEG-PBA-PEG	SPION-PEG-PBA-PEG-FA
OLN-93	64.36 ± 2.3	67.7 ± 1.57
C6	62.3 ± 2.2	157.39 ± 3.4

respectively (Table 2).

3.3.3. *In vitro TMZ release profiles*

The in vitro cumulative release profiles of TMZ from TMZ-SPION-PEG-PBA-PEG and TMZ-SPION-PEG-PBA-PEG-FA at 37 °C and pH = 7.4 have been shown in Fig. 2G. Before conducting these release assays, TMZ release profile from stock solution was considered as positive control. It was found that nearly 90% of TMZ in stock solution was released within the first 2 h (Fig. 2G). When TMZ loaded into NPs, we observed a bi-phasic release pattern for TMZ which was characterized by an initial burst release, followed by a sustained drug release. The initial fast drug release of 48.3 ± 1.7% and 45.9 ± 2.8% within 4 h was observed for TMZ-SPION-PEG-PBA-PEG and FA-conjugated NPs, respectively. After 48 h, the cumulative release was 76.13 ± 2.3% for TMZ-SPION-PEG-PBA-PEG and 74.43 ± 0.77% for TMZ-SPION-PEG-PBA-PEG-FA. We could conclude that TMZ-loaded NPs had a sustained release feature, which might be described that the drug was gradually released with the dissolution of polymers.

3.4. *Cell experiments*

3.4.1. *Cellular uptake of NPs*

The internalization of the NPs into cells and the targeting effects of the FA-conjugated NPs were assessed using the Prussian blue staining and the ICP-OES analysis by C6 rat glioblastoma (FA-receptor positive) and OLN-93 rat glial (FA-receptor negative) cell lines after 2 h and 24 h incubation with NPs. The uptake of nanoparticles in both cell lines was confirmed by qualitative images of the Prussian blue staining (Fig. 3A-H). Furthermore, the cellular uptake of all NPs in both cells was time-dependent.

The quantitative ICP-OES data were shown in Table 3. The cellular uptake of Fe after 24 h incubation with SPION-PEG-PBA-PEG was equal to 64.36 ± 2.3 and 62.3 ± 2.2 pg/cell for OLN-93 and C6, respectively. Whereas, for SPION-PEG-PBA-PEG-FA (at the same concentrations of Fe_3O_4) was increased to 67.7 ± 1.57 and 157.39 ± 3.4 pg/cell, respectively. Our results suggested the improving internalization of SPION-PEG-PBA-PEG-FA into C6 cells compared to OLN-93. Also, the C6 cell uptake of FA-conjugated NPs was 2.5-fold higher than that of unmodified NPs ($P < 0.0001$).

3.4.2. *In vitro cytotoxicity assay*

It is necessary to assess the cytotoxicity of the synthesized NPs before further biomedical applications. Therefore, the MTT assay was used to evaluate the cytotoxicity of free drug and different NPs formulations. The viability of both cells incubated with different concentrations of TMZ and four types of NPs (at the same concentration of TMZ) has been showed in Fig. 4. As it can be seen in Fig. 4, TMZ and all NPs showed a significant increase in cytotoxicity as the concentration increased.

The IC50 values of TMZ, TMZ-SPION-PEG-PBA-PEG, and TMZ-SPION-PEG-PBA-PEG-FA after 24 h treatment (Figure 4A&B) were equal to 137.6 ± 2.2, 83.4 ± 0.62, and 43.3 ± 0.72 μg/mL for C6 cells and 104.7 ± 0.95, 70.7 ± 1.1, and 75.7 ± 1.25 μg/mL for OLN-93 cells, respectively. However, after 48 h treatment (Figure 4C&D), the IC50 values of TMZ, TMZ-SPION-PEG-PBA-PEG, and TMZ-SPION-PEG-PBA-PEG-FA were decreased to 133.1 ± 1.02, 62.5 ± 0.8, and 26.3 ± 1.1 μg/mL for C6 cells and 102.8 ± 0.5, 54.3 ± 1.2, and 56.5 ± 1.05 μg/mL for OLN-93 cells, respectively.

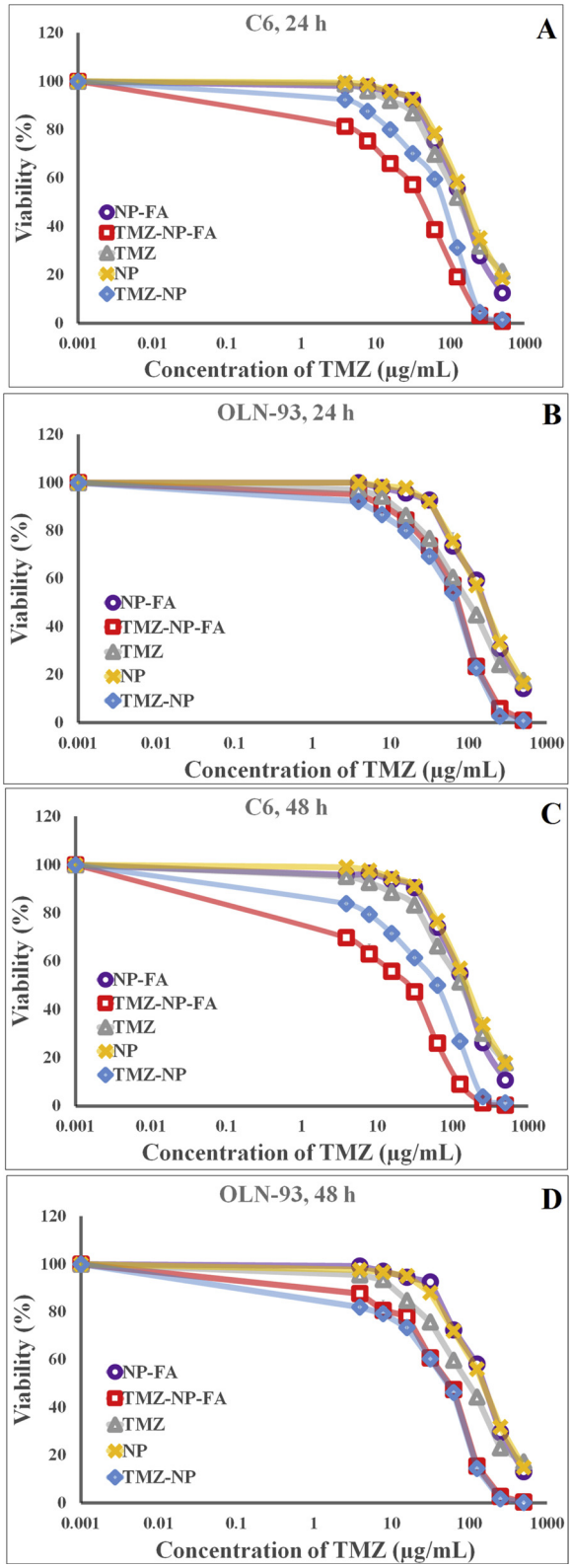

Fig. 4. In vitro anti-proliferative effect in C6 and OLN-93 cells after treatment with various concentrations of TMZ alone and different formulations of NPs for 24 h (A&B) and 48 h (C&D) was evaluated by the MTT assay (NP means SPION-PEG-PBA-PEG).

The results from MTT assay indicated that after 24 and 48 h

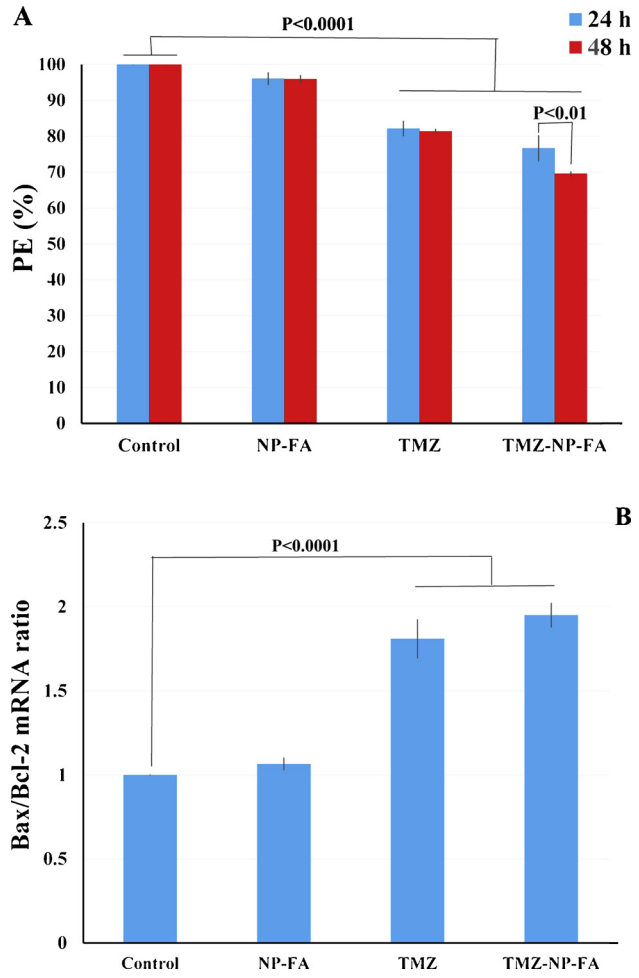

Fig. 5. (A) In vitro antitumor performance of TMZ, NP-FA, and TMZ-NP-FA in C6 cells after 24 and 48 h treatment was evaluated by the colony formation assay. (B) The qRT-PCR analysis in C6 cells treated with TMZ, NP-FA, and TMZ-NP-FA for 24 h (NP means SPION-PEG-PBA-PEG). Data were represented mean ± SD (n = 3).

treatment the TMZ-SPION-PEG-PBA-PEG-FA NPs revealed the highest anti-proliferation ability on C6 cells compared to OLN-93 cells ($P < 0.0001$). In addition, the cytotoxicity of TMZ-SPION-PEG-PBA-PEG-FA after 24 and 48 h treatment was 2 and 2.37-fold higher than that of TMZ-SPION-PEG-PBA-PEG on C6 cells, respectively ($P < 0.0001$), which demonstrated a satisfactory drug delivery system.

Furthermore, in order to confirm the absence of cytotoxic effects of the NPs without the drug, the MTT assay was also performed for the blank NPs (SPION-PEG-PBA-PEG and SPION-PEG-PBA-PEG-FA). As shown in Fig. 4A-D, the cytotoxic effects of blank NPs were insignificant. The cell viability was above 90% at the concentration of 800 μg/mL (equivalent to TMZ-loaded NPs containing about 35.2 μg/mL of TMZ) in the 24 and 48 h treatment. This represented the safety of polymers and other excipients used for fabricating the NPs.

Based on these observations, IC_{10} concentration (21.71 μg/mL) of TMZ in free and loaded form was selected for further studies as a suitable concentration on C6 cells.

3.4.3. *In vitro anti-tumor efficacy of nanoparticles*

3.4.3.1. Colony formation assay. Anti-proliferative activity of 111.7 μM TMZ (21.7 μg/mL), 0.493 μg/mL TMZ-SPION-PEG-PBA-PEG-FA (containing 111.7 μM TMZ), and SPION-PEG-PBA-PEG-FA (0.493 μg/mL) on C6 cells was evaluated using the clonogenic assay. As shown in Fig. 5A, the Plating Efficiency (PE) of SPION-PEG-PBA-PEG-FA after 24 and 48 h treatment had no significant difference with control cells ($P > 0.05$) which indicated that the blank NPs possessed excellent cytocompatibility. The plating efficiency of TMZ alone and TMZ-SPION-PEG-PBA-PEG-FA after 24 h treatment was equal to 82.14 ± 2.04% and 76.6 ± 3.4%, respectively. After 48 h treatment, the plating efficiency of TMZ-SPION-PEG-PBA-PEG-FA was decreased to 69.6 ± 0.5% ($P < 0.01$). However, for C6 cells treated with TMZ alone there was no statistically significant difference between the plating efficiency of 24 and 48 h treatment. It was found that the cytotoxicity of TMZ incorporated FA-conjugated NPs on C6 cells after 24 and 48 h treatment was significantly higher than that of pure TMZ ($P < 0.05$).

3.4.3.2. Quantitative real-time PCR. The expression of Bcl_2 family members that code for proteins involved in mitochondrial apoptotic pathway following 24 h of treatment with TMZ alone, TMZ-SPION-PEG-PBA-PEG-FA, or SPION-PEG-PBA-PEG-FA was analyzed from total RNA of C6 cells through the qRT-PCR assay, and Bax/Bcl2 mRNA ratio was evaluated (Fig. 5B). As it has been shown in Fig. 5B, Bax/Bcl2 mRNA ratio was increased noticeably in TMZ and TMZ-loaded NPs as compared to untreated cells ($P < 0.0001$). However, no significant changes were observed between the control group and the blank NPs ($P > 0.05$). Our results revealed that TMZ-SPION-PEG-PBA-PEG-FA NPs significantly increased Bax/Bcl2 mRNA ratio in comparison with TMZ alone ($P < 0.01$).

3.4.3.3. Cell apoptosis assay. In our study, the Annexin V-FITC/PI double fluorescent staining assay was used to identify the apoptosis and necrosis of C6 glioma cells. Results of flow cytometry analysis has been shown in Fig. 6. As determined by flow cytometry analysis, there was a significant difference between the control group and TMZ, TMZ-SPION-PEG-PBA-PEG-FA groups ($P < 0.0001$). The significant difference in the cell death ratio was also observed between TMZ alone and TMZ-loaded NPs ($P < 0.0001$). As it can be seen in Fig. 6B, the highest apoptosis and necrosis level (15.25%) was related to TMZ-SPION-PEG-PBA-PEG-FA group. In addition, there were no significant differences between the control group and blank NPs ($P > 0.05$), also the blank NPs showed the minimal apoptosis. The result of flow cytometry analysis was in complete agreement with the molecular research.

4. Discussion

In this study, we succeeded to synthesize four types of NPs which had many advantages such as protecting degradation of drug, releasing a therapeutic payload in the optimal dosage range, and targeted delivery using the FA-ligand.

The average size of all NPs was below 50 nm that were regarded to be favorable for cell transport. After decorating NPs with FA-ligand, the size of SPION-PEG-PBA-PEG and TMZ-SPION-PEG-PBA-PEG was found to be increased slightly (from 24.82 to 27.33 and from 44 to 48.6 nm, respectively). This could be due to the presence of FA molecules at the surface of NPs which caused to increase the size. This result was in agreement with other studies (Hu et al., 2013a, b). Additionally, loading TMZ into NPs also led to an increase in size which was similar to the results published by Ebrahimi Shahmabadi et al (Shahmabadi et al., 2014), who showed that loading Cisplatin into NPs caused to an increase in size from 373 to 489 nm.

It was found that more than 90% of TMZ was released within the first 2 h. This finding could be correlated with a half-life of the drug which was 1.8 h (Tsang et al., 1990). However, when the drug was loaded into NPs, its half-life was prolonged as indicated in the release profile.

In the first 4 h, a burst release of TMZ was obtained from both NPs which probably derived from the fraction of the drug located on the surface of NPs and poorly encapsulated in the polymer. After that, the release rate decreased with time and sustained release was presented.

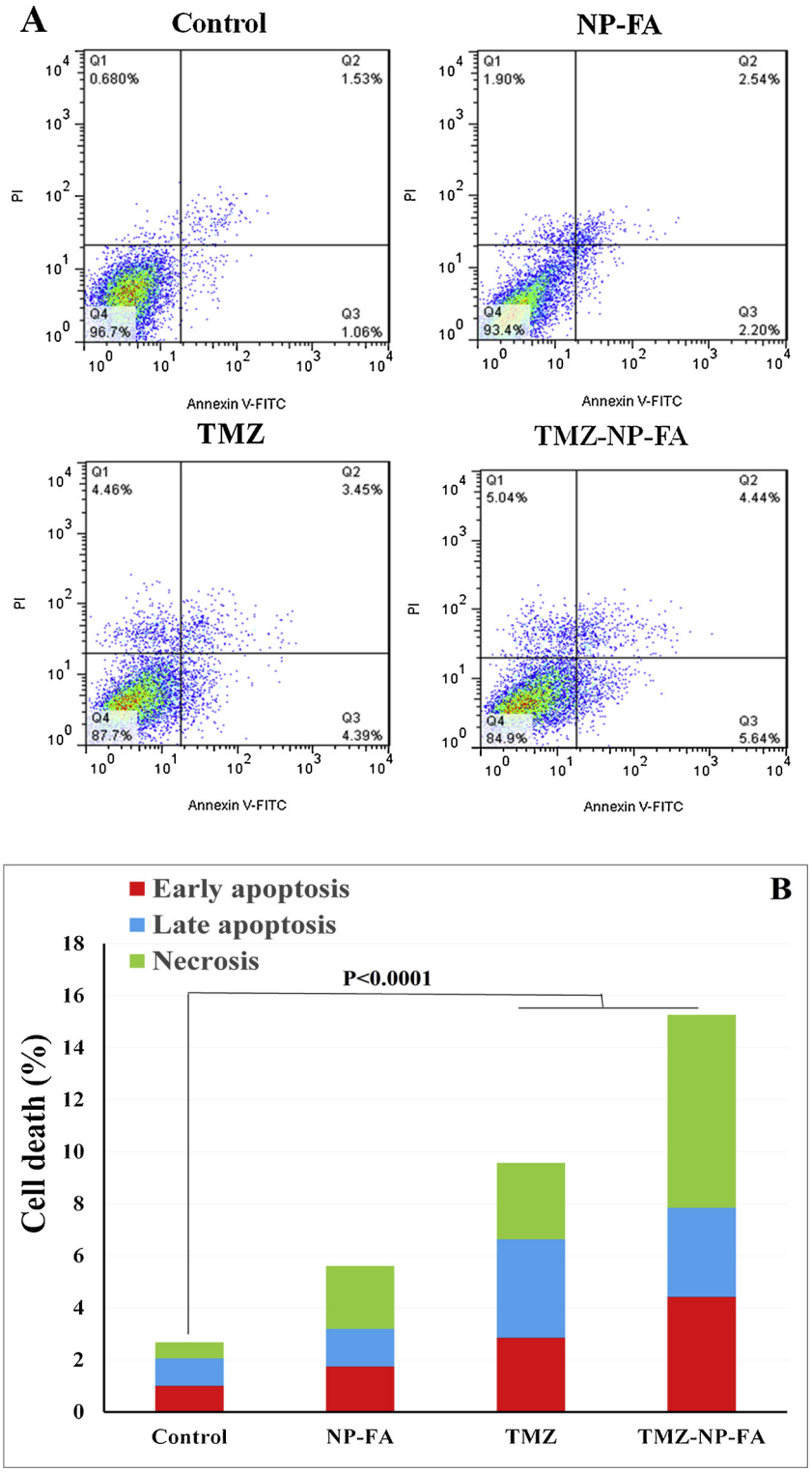

Fig. 6. (A) The Annexin-V/PI double-staining assay for detecting the apoptosis of C6 cells. (B) The percentage of necrosis and apoptosis of C6 cells after treatment with 21.7 μg/mL TMZ, 0.493 mg/mL NP-FA, and 0.493 mg/mL TMZ-NP-FA (containing 21.7 μg/mL TMZ) for 24 h (mean ± SD, n = 3) (NP means SPION-PEG-PBA-PEG).

This sustained release was attributed to the incorporated TMZ in the nanoparticle core and released in a prolonged way along with degradation of the triblock copolymers. (Xu et al. (2016)) reported that about 82% of loaded TMZ was released from the TMZ-mPEG-PLGA NPs within 24 h. While, in our study, the cumulative release was less than 77% within 48 h. Thus, our NPs revealed a sustained release feature in comparison with that.

C6 glioma cells and OLN-93 glial cells were used to identify the targeting effect of the NPs with FA. In this experiment, the qualitative and quantitative analysis demonstrated that SPION-PEG-PBAPEG-FA nanoparticles could target C6 cells.

As shown in Table 3, the cellular uptake of SPION-PEG-PBAPEG-FA in C6 cells was 2.32-fold higher than that of OLN-93 cells ($P < 0.0001$). Furthermore, folic acid conjugation could improve the

internalization of NPs into C6 cells. For FA-conjugated NPs, the cellular association was increased to be 2.5-fold higher than that of NPs without FA ($P < 0.0001$). These results were due to the expression of FA-receptor on the surface of C6 cells (Saul et al., 2003) that led to the transportation of NPs into the cells through receptor-mediated endocytosis, which was in line with other studies (Kuo and Chen, 2015; Lu et al., 2012).

It was straightforward to comprehend that both the concentration and the time of treatment had a major role in the cytotoxicity of TMZ-loaded nanoparticles. However, there was no significant difference in the cytotoxicity of TMZ alone between 24 and 48 h treatment in both cell lines ($P > 0.05$). After 24 h treatment, the cell viability of TMZ-loaded NPs (with or without FA) in both cells was lower than that of TMZ alone ($P < 0.0001$). Increasing the treatment time for more than 48 h induced more cytotoxicity of TMZ-loaded NPs, but the anti-proliferative effect of TMZ alone was not increased. This could be due to short half-life and instability of TMZ. The drug was degraded very quickly in the culture media and lost its potency, but TMZ-loaded NPs revealed a continuous release during the treatment. The result was also in agreement with the other studies (Zhang et al., 2012; Jain et al., 2013). Furthermore, the cytotoxicity effect of TMZ-loaded FA-conjugated NPs in C6 cells during 24 and 48 h treatment was 3.2 and 5-fold higher than that of TMZ alone, which indicated that the half-life of TMZ could be extended by loading the drug into nanoparticles.

The anti-proliferative effect of TMZ alone and TMZ-SPION-PEG-PBA-PEG NPs in OLN-93 cells within 24 and 48 h incubation was significantly higher than that of C6 cells ($P < 0.0001$). Whereas, the cytotoxicity effect of TMZ-loaded FA-conjugated NPs in C6 cells after 24 and 48 h incubation was 1.75 and 2.14-fold higher than that of OLN-93 cells, respectively ($P < 0.0001$), which demonstrated a satisfactory targeted drug delivery system due to the expression of FA-receptor on the surface of C6 cells. Kuo et al. (Kuo and Chen, 2015) showed that the order in the anti-proliferative effect in U87MG cells was Lf-FA-PLGA > FA-PLGA > PLGA > etoposide alone. In their study, FA could target the FA-receptor expressed by U87MG cells.

Further studies showed that the IC_{50} value of TMZ-SPION-PEG-PBAPEG-FA in C6 cells after 24 and 48 h treatment was 2 and 2.37 times lower than that of TMZ-SPION-PEG-PBA-PEG, respectively ($P < 0.0001$), while such effect was not observed in the case of OLN-93 cells. The anti-proliferative results were in accordance with the cellular uptake data, demonstrating that FA-conjunction could significantly improve C6 cellular association and anti-glioma efficacy.

In all analysis, there was no noticeable difference between the SPION-PEG-PBA-PEG-FA NPs and the control groups ($P > 0.05$), which illustrated the biocompatibility and nontoxicity of nanoparticles without the drug.

The results of colony formation assay indicated that C6 cells lost the ability to replicate in the presence of TMZ or TMZ-SPION-PEG-PBA-PEG-FA NPs in comparison with untreated cells ($P < 0.0001$). However, the effect of TMZ-SPION-PEG-PBA-PEG-FA was higher than that of TMZ alone after 24 ($P < 0.05$) and 48 h treatment ($P < 0.0001$), which could be due to the sustain release effect of NPs and satisfactory targeted drug delivery system. (Zhao et al. (2012)) evaluated the anti-proliferation activity of PTX encapsulated NPs by the MTT assay in Hela and A549 cells. In folic receptor-positive Hela cells, the cytotoxicity of PTX-loaded FLPNPs was higher than that of PTX-loaded LPNPs or Taxol alone. On the contrary, in the folic receptor-negative A549 cells, there was no significant difference between the PTX-loaded FLPNPs, PTX-loaded LPNPs, and Taxol alone. They found that PTX-loaded FLPNPs had a higher drug efficacy than Taxol, and the anticancer activity was due to targeted drug delivery.

In this study, the improved intracellular drug delivery following FA-conjugation was further confirmed using the qRT-PCR assay. In C6 cells, a decrease in Bcl2 mRNA expression and an increase in Bax mRNA expression were observed in TMZ alone and TMZ-SPION-PEG-PBA-PEG-FA NPs groups. However, the Bax/Bcl2 ratio of TMZ-SPION-PEG-PBA-PEG-FA NPs was higher than that of TMZ alone ($P < 0.0001$). Members of the Bcl2 family are critical mediators of the apoptotic process. The Bax/Bcl2 ratio is the key factor that activates the mitochondrial pathway of apoptosis, and when the ratio of Bax/Bcl2 increases apoptosis is initiated (Roset et al., 2007).

The results of the flow cytometry analysis were in a good agreement with qRT-PCR analysis, indicating that TMZ-SPION-PEG-PBA-PEG-FA NPs could induce the highest early and late apoptosis and necrosis level (15.25%) due to the targeting effect and the high accumulation of TMZ in C6 cells via an FA receptor-mediated endocytosis. Hu et al. reported that the percentage of apoptotic C6 cells untreated and treated with the Taxol, NP-PTX, and tLyp-1-NP-PTX was 3.4 ± 0.45%, 9.21 ± 1.67%, 8.85 ± 1.35%, and 20.6 ± 3.32%, respectively (Hu et al., 2013b). Their results indicated that tLyp-1-NP-PTX led to more apoptosis compared to other PTX-formulations, because tLyp-1 peptide was a ligand-targeted to the Neuropilin receptors that were over-expressed on the surface of C6 cells, and led to transport into the cells.

5. Conclusion

In this study, TMZ-loaded magnetite triblock copolymers were synthesized, which were modified with tumor-targeting ligand (FA). C6 glioma cells experiments treated with TMZ alone or different NPs formulations in vitro supported the utility of FA-ligand as a drug delivery platform to target C6 cells through the expression of FA-receptors on the surface of C6 cells. Therefore, synthesized NPs could be used as a potential carrier for targeted delivery of the drug to C6 glioma cells.

Conflict of interest

The authors report no conflicts of interest. The authors alone are responsible for the content and writing of the paper.

Acknowledgment

This work was supported by grant No. 29706 from Iran University of Medical Sciences (IUMS).

References

Asadi, L., Shirvalilou, S., Khoee, S., Khoei, S., 2018. Cytotoxic effect of 5-Fluorouracil-loaded polymer-coated magnetite nanographene oxide combined with radiofrequency. Anticancer Agents Med. Chem.

Baker, S.D., Wirth, M., Statkevich, P., Reidenberg, P., Alton, K., Sartorius, S.E., et al., 1999. Absorption, metabolism, and excretion of 14C-temozolomide following oral administration to patients with advanced cancer. Clin. Cancer Res. 5 (2), 309–317.

Cheng, W., Nie, J., Xu, L., Liang, C., Peng, Y., Liu, G., et al., 2017. pH-Sensitive delivery vehicle based on folic acid-conjugated polydopamine-modified mesoporous silica nanoparticles for targeted cancer therapy. ACS Appl. Mater. Interfaces 9 (22), 18462–18473.

Cherukuri, P., Glazer, E.S., Curley, S.A., 2010. Targeted hyperthermia using metal nanoparticles. Adv. Drug Deliv. Rev. 62 (3), 339–345.

Erdoğar, N., Esendağlı, G., Nielsen, T.T., Esendağlı-Yılmaz, G., Yöyen-Ermiş, D., Erdoğdu, B., et al., 2018. Therapeutic efficacy of folate receptor-targeted amphiphilic cyclodextrin nanoparticles as a novel vehicle for paclitaxel delivery in breast cancer. J. Drug Target. 26 (1), 66–74.

Furnari, F.B., Fenton, T., Bachoo, R.M., Mukasa, A., Stommel, J.M., Stegh, A., et al., 2007. Malignant astrocytic glioma: genetics, biology, and paths to treatment. Genes Dev. 21 (21), 2683–2710.

Gladson, C.L., Prayson, R.A., Liu, W.M., 2010. The pathobiology of glioma tumors. Annu. Rev. Pathol. Mech. Disease. 5, 33–50.

Hadjipanayis, C.G., Machaidze, R., Kaluzova, M., Wang, L., Schuette, A.J., Chen, H., et al., 2010. EGFRvIII antibody–conjugated iron oxide nanoparticles for magnetic resonance imaging–guided convection-enhanced delivery and targeted therapy of glioblastoma. Cancer Res. 70 (15), 6303–6312.

Hu, Q., Gu, G., Liu, Z., Jiang, M., Kang, T., Miao, D., et al., 2013a. F3 peptide-functionalized PEG-PLA nanoparticles co-administrated with tLyp-1 peptide for anti-glioma drug delivery. Biomaterials. 34 (4), 1135–1145.

Hu, Q., Gao, X., Gu, G., Kang, T., Tu, Y., Liu, Z., et al., 2013b. Glioma therapy using tumor homing and penetrating peptide-functionalized PEG–PLA nanoparticles loaded with paclitaxel. Biomaterials 34 (22), 5640–5650.

Jaimes-Aguirre, L., Morales-Avila, E., Ocampo-García, B.E., Medina, L.A., López-Téllez, G., Gibbens-Bandala, B.V., et al., 2017. Biodegradable poly (D, L-lactide-co-

glycolide)/poly (L-γ-glutamic acid) nanoparticles conjugated to folic acid for targeted delivery of doxorubicin. Mater. Sci. Eng. C 76, 743–751.
Jain, D.S., Athawale, R.B., Bajaj, A.N., Shrikhande, S.S., Goel, P.N., Nikam, Y., et al., 2013. Poly lactic acid (PLA) nanoparticles sustain the cytotoxic action of temozolomide in C6 Glioma cells. Biomed. Aging Pathol. 3 (4), 201–208.
Kargar, S., Khoei, S., Khoee, S., Shirvalilou, S., Mahdavi, S.R., 2018. Evaluation of the combined effect of NIR laser and ionizing radiation on cellular damages induced by IUdR-loaded PLGA-coated nano-graphene oxide. Photodiagn. Photodyn. Ther. 21, 91–97.
Karlsson, J., Vaughan, H.J., Green, J.J., 2018. Biodegradable polymeric nanoparticles for therapeutic cancer treatments. Annu. Rev. Chem. Biomol. Eng.(0).
Khoee, S., Bagheri, Y., Hashemi, A., 2015. Composition controlled synthesis of PCL–PEG Janus nanoparticles: magnetite nanoparticles prepared from one-pot photo-click reaction. Nanoscale 7 (9), 4134–4148.
Khoei, S., Azarian, M., Khoee, S., 2012. Effect of hyperthermia and triblock copolymeric nanoparticles as quercetin carrier on DU145 prostate cancer cells. Curr. Nanosci. 8 (5), 690–696.
Kim, W.Y., Lee, H.Y., 2009. Brain angiogenesis in developmental and pathological processes: mechanism and therapeutic intervention in brain tumors. FEBS J. 276 (17), 4653–4664.
Kuo, Y.-C., Chen, Y.-C., 2015. Targeting delivery of etoposide to inhibit the growth of human glioblastoma multiforme using lactoferrin-and folic acid-grafted poly (lactide-co-glycolide) nanoparticles. Int. J. Pharm. 479 (1), 138–149.
Lu, Y.-J., Wei, K.-C., C-CM, Ma, Yang, S.-Y., Chen, J.-P., 2012. Dual targeted delivery of doxorubicin to cancer cells using folate-conjugated magnetic multi-walled carbon nanotubes. Colloids Surf. B Biointerfaces 89, 1–9.
Miura, Y., Takenaka, T., Toh, K., Wu, S., Nishihara, H., Kano, M.R., et al., 2013. Cyclic RGD-linked polymeric micelles for targeted delivery of platinum anticancer drugs to glioblastoma through the blood–brain tumor barrier. ACS Nano 7 (10), 8583–8592.
Mohammadi Gazestani, A., Khoei, S., Khoee, S., Emamgholizadeh Minaei, S., Motevalian, M., 2018. In vivo evaluation of the combination effect of near-infrared laser and 5-fluorouracil-loaded PLGA-coated magnetite nanographene oxide. Artif. Cells Nanomed. Biotechnol. 1–9.
Mustafa, T., Zhang, Y., Watanabe, F., Karmakar, A., Asar, M.P., Little, R., et al., 2013. Iron oxide nanoparticle-based radio-frequency thermotherapy for human breast adenocarcinoma cancer cells. Biomater. Sci. 1 (8), 870–880.
Özcan, I., Segura-Sanchez, F., Bouchemal, K., Sezak, M., Özer, Ö, Güneri, T., et al., 2010. Pegylation of poly (γ-benzyl-L-glutamate) nanoparticles is efficient for avoiding mononuclear phagocyte system capture in rats. Int. J. Nanomedicine 5, 1103.
Reni, M., Mason, W., Zaja, F., Perry, J., Franceschi, E., Bernardi, D., et al., 2004. Salvage chemotherapy with temozolomide in primary CNS lymphomas: preliminary results of a phase II trial. Eur. J. Cancer 40 (11), 1682–1688.
Roset, R., Ortet, L., Gil-Gomez, G., 2007. Role of Bcl-2 family members on apoptosis: what we have learned from knock-out mice. Front Biosci. 12 (20), 4722–4730.
Rychahou, P., Bae, Y., Reichel, D., Zaytseva, Y.Y., Lee, E.Y., Napier, D., et al., 2018. Colorectal cancer lung metastasis treatment with polymer–drug nanoparticles. J. Control. Release 275, 85–91.
Sarin, H., 2009. Recent progress towards development of effective systemic chemotherapy for the treatment of malignant brain tumors. J. Transl. Med. 7 (1), 77.
Saul, J.M., Annapragada, A., Natarajan, J.V., Bellamkonda, R.V., 2003. Controlled targeting of liposomal doxorubicin via the folate receptor in vitro. J. Control. Release 92 (1-2), 49–67.
Shahmabadi, H.E., Movahedi, F., Esfahani, M.K.M., Alavi, S.E., Eslamifar, A., Anaraki, G.M., et al., 2014. Efficacy of Cisplatin-loaded polybutyl cyanoacrylate nanoparticles on the glioblastoma. Tumor Biol. 35 (5), 4799–4806.
Shanavas, A., Sasidharan, S., Bahadur, D., Srivastava, R., 2017. Magnetic core-shell hybrid nanoparticles for receptor targeted anti-cancer therapy and magnetic resonance imaging. J. Colloid Interface Sci. 486, 112–120.
Tsang, L.L., Farmer, P.B., Gescher, A., Slack, J.A., 1990. Characterisation of urinary metabolites of temozolomide in humans and mice and evaluation of their cytotoxicity. Cancer Chemother. Pharmacol. 26 (6), 429–436.
Tsang, L.L., Quarterman, C.P., Gescher, A., Slack, J.A., 1991. Comparison of the cytotoxicity in vitro of temozolomide and dacarbazine, prodrugs of 3-methyl-(triazen-1-yl) imidazole-4-carboxamide. Cancer Chemother. Pharmacol. 27 (5), 342–346.
Wen, P.Y., Kesari, S., 2008. Malignant gliomas in adults. N. Engl. J. Med. 359 (5), 492–507.
Xu, Y., Shen, M., Li, Y., Sun, Y., Teng, Y., Wang, Y., et al., 2016. The synergic antitumor effects of paclitaxel and temozolomide co-loaded in mPEG-PLGA nanoparticles on glioblastoma cells. Oncotarget. 7 (15), 20890.
Zhang, D., Tian, A., Xue, X., Wang, M., Qiu, B., Wu, A., 2012. The effect of temozolomide/poly (lactide-co-glycolide)(PLGA)/nano-hydroxyapatite microspheres on glioma U87 cells behavior. Int. J. Mol. Sci. 13 (1), 1109–1125.
Zhao, P., Wang, H., Yu, M., Liao, Z., Wang, X., Zhang, F., et al., 2012. Paclitaxel loaded folic acid targeted nanoparticles of mixed lipid-shell and polymer-core: in vitro and in vivo evaluation. Eur. J. Pharm. Biopharm. 81 (2), 248–256.